22nd International Conference on Renewable Energies and Power Quality (ICREPQ'24)
Bilbao (Spain), 26th to 28th June 2024

ISBN: 978-84-09-60656-6

Five-phase Inverter Control Based on the Haar Wavelet Transform

J. Iwaszkiewicz[1] and A. Muc[1]

[1] Department of Ship Automation
Gdynia Maritime University
Morska St. 83, 81-225 Gdynia (Poland)
Phone/Fax number:+48 505 279 861

Abstract. The paper presents a novel five-phase cascade inverter control method based on the Haar wavelets transform. The inverter is built from two or three two level inverters in every phase. The instantaneous value of the output voltage of the cascaded inverter is composed as a synthesis of the selected Haar wavelets. An analytical system of determining the best possible set of Haar orthogonal wavelets is presented. On the basis of the applied Haar wavelets, the control signals of the inverter switches are calculated. The cascaded five-phase inverter with a star connected resistive-inductive load was tested during simulation tests. The results and discussion of main proprieties are presented.

Keywords. Wavelets, Haar wavelet transform, wavelet waveforms synthesis, five-phase multilevel inverter.

1. Introduction

Over the past few decades, inverters have become a popular technology. The great interest in optimizing and improving the efficiency of inverters is justified by the continuous demand for their use in various industry sectors, such as electric drives, power systems, and renewable energy systems. One of the goals of this research effort is to develop and experimentally test electronic key-switching techniques that allow the control of inverters to produce input signals with reduced harmonic content, regardless of their ratings, configurations, types, and load conditions. Several inverter-switching techniques have been described in the literature and have been developed and tested to support both single-phase and three-phase inverters [1, 2, 3].

Devices such as voltage and current converters are now able to control and power a variety of devices operating in the power range of hundreds of kW and more. These devices have to fulfil definite and diversified requirements which implies diversified purposes and methods of electric energy conversion. There are many industrial applications e.g. uninterruptible power supplies (UPS) or distributed power generation systems, where the essential demand is to generate 50 or 60 Hz sinusoidal voltage waveforms. The quality of generated waveforms, especially the Total Harmonic Distortion factor (THD), should comply with appropriate standards. In many devices like UPSs, active filters, or voltage regulators in electric energy grids, the most important features are high-quality output waveforms, output stability, and efficiency of the device. Similar requirements are to be fulfilled in converters applied in renewable energy systems.

Recently, multilevel inverters have emerged as a new and very important class of converters. Thanks to their promising performance, multilevel inverters are becoming more and more an alternative to conventional two-level inverters. They permit us to overcome the problem of limited power and shape output waveforms. As a result, many multilevel converters have been applied in the industry.

The development of multilevel converters comprises a novel area of research for new topologies, control strategies, and theory. Producing the required voltage or current waveforms is possible in many ways: e.g. sinusoidal PWM, selective harmonic elimination, space-vector modulation (SVM), or shaping the stepped voltage or current [4, 5, 6, 7]. Important works and studies concern the subject of increased number of inverter levels [8, 9]. Diverse control methods such as computing the adequate switching angles of stepped waveforms or cutting specified harmonics have been developed.
The disadvantages of numerous fast switching states can be slightly reduced by the use of novel converters topologies as well as mathematical tools-aided control strategies. One of the promising theory is based on orthogonal vectors arrangement. The proposal of the modified control relates to the idea of a converter based on the orthogonal vector theory. The basic structure of the converter consists of two conventional two-level inverters where two adequate orthogonal vectors are summing. The resulting in converter output waveforms form a stepped voltage and its THD factor is relatively low [10, 11, 12, 13, 14]. Another proposal permitting to obtain stepped voltage waveforms can be achieved by use of cascaded inverters built from two or more number of two level inverters. A cascaded multilevel inverter based on switched capacitor is presented in [15]. The paper deals with an original technique of shaping the stepped output waveforms in multilevel cascaded converters. The control idea is based on wavelets' transform. The Haar wavelet transform has been selected as a very suitable mathematical tool enabling to realize this task. The output waveform synthesis is accomplished using a set of orthogonal Haar wavelets [16]. The article presents the initial simulation studies of the three-phase inverter model controlled by wavelet signals. This is the first inverter

model that enables the implementation of the wavelet theory. The next step will be an attempt to implement the presented inverter and experimental research.

2. Wavelet waveforms synthesis

Wavelets is a term for mathematical functions, that allow the analysis of signals in different time scales and resolutions. The wavelet applications are in many not directly related areas like seismology, video analysis, quantum mechanics, or electronics. The wavelets have been used mainly for analysing processes or signals based on the decomposition of the elements of the processes. The following considerations will prove that wavelets can also be useful in the composition of power electronics signals and structures. The main application of the wavelet theory is used in control algorithms [10,11,12,13] or diagnostics [14,15] and the detection [16] of various types of faults in converters, networks, or drives [2]. The Haar wavelet, on the other hand, is not so widely used.

The Haar wavelets have been adapted [6,7] for cascade inverter control. The Haar wavelet form is similar to the form of the voltage or current pulse that can be obtained using a simple one-phase inverter i.e. H-bridge cell. The displacement and width of the wavelet can be freely created and controlled. Thanks to these properties it is possible to apply wavelets in power electronics e.g. to form the output stepped waveforms of multilevel converters [16].

Let us define the scaling function $\varphi(x)$ in an interval $x \in <0,2\pi)$:

$$\varphi(x) = \begin{cases} 1 & \text{for} \quad 0 \le x < 2\pi, \\ 0 & \text{for} \quad \text{other} \quad x \end{cases} \tag{1}$$

The fundamental proposed wavelet is defined:

$$\psi(x) = \begin{cases} 1 & \text{for} \quad 0 \le x < \pi, \\ -1 & \text{for} \quad \pi \le x < 2\pi, \\ 0 & \text{for} \quad \text{other} \quad x \end{cases} \tag{2}$$

The wavelet determines one period of the rectangular wave and is the mother function introducing a family of wavelets:

$$\psi_{mn}(x) = \psi\left(2^{-m}x - 2\pi n\right) \quad \text{for} \quad m, n = ..., -2, -1, 0, 1, 2, ... \tag{3}$$

The wavelet scale is done as $2^m 2\pi$ and its displacement on the x-axis is determined as n-times $2^{m+1}\pi$. The m factor scales not only the wavelet but the amplitude too.

The scaling function and a few wavelets have been presented in Figure 1.

All wavelets $\psi_{mn}(x)$ are orthogonal in the interval $x \in <0,2\pi)$. The defined statement (7) creates a family of orthogonal functions and can determine the basis of the wavelet transform. A continuous wavelet transform is defined as:

$$Wf(m,n) = \int_{-\infty}^{\infty} f(x)\psi_{mn}(x)\,\mathrm{d}x \tag{4}$$

and presents itself as a scalar product of functions $f(x)$ and function $\psi_{mn}(x)$. The function f(x) reconstruction occurs when the inverse wavelet transform is applied (5).

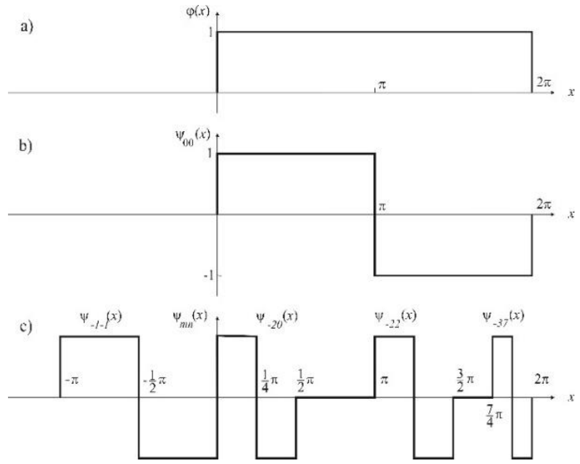

Fig.1. The scaling function $\varphi(x)$ and wavelets $\psi_{mn}(x)$: a) scaling function $\varphi(x)$, b) fundamental wavelet $\psi_{00}(x)$, c) wavelets $\psi_{-1-1}(x)$, $\psi_{-20}(x)$, $\psi_{-22}(x)$, $\psi_{-37}(x)$.

In applications more comfortable is using a discrete inverse wavelet transform which is defined according to (6) by the equation:

$$f(x) = C\sum_{m=-\infty}^{\infty}\sum_{n=-\infty}^{\infty} Wf(m,n)\,\psi_{mn}(x) \tag{5}$$

The symbol C denotes a constant that can be calculated from the Fourier transform of the function $\psi_{mn}(x)$. It could be written as a sum of wavelets $\psi_{mn}(x)$ multiplied by coefficients a_{mn}

$$f(x) = \sum_{m=-\infty}^{\infty}\sum_{n=-\infty}^{\infty} a_{mn}\,\psi_{mn}(x) \tag{6}$$

The coefficients a_{mn}, called wavelet coefficients, are scalar products of the function $f(x)$ and wavelets $\psi_{mn}(x)$. In the interval $x \in <0,2\pi)$ they are given as

$$a_{mn} = C_m \int_0^{2\pi} f(x)\psi_{mn}(x)\,\mathrm{d}x \tag{7}$$

The constant C_m is only dependent on coefficient m and has the same value for different n. Denoting

$$f_{mn}(x) = a_{mn}\,\psi_{mn}(x) \tag{8}$$

it is possible to write $f_\psi(x)$ as a sum of components $f_{mn}(x)$:

$$f_\psi(x) = \sum_{m=-3}^{m=0}\sum_{n=0}^{2^{-m}-1} f_{mn}(x) \tag{9}$$

The components are $f_{mn}(x)$ present component wavelets, amplitude, and phase which are determined by coefficients a_{mn}, calculated according to (7).

In power electronics, the most important criterion of the approximated waveforms is the THD factor. Practically in power electronics applications, the approximation of a sine wave should be realized using a finite number of wavelets. The natural aspiration of designers is to utilize the possibly lowest number of components. The accuracy of approximation depends on it. In mathematics, the accuracy is determined as an average square error δ, a very useful criterion destined for that purpose.

Let us denote by $f_{\psi}(x)$ a waveform approximating the function $f(x)=\sin(x)$ in the interval $x \in <0, 2\pi)$. Assuming that $f_{\psi}(x)$ forms a combination of wavelets determined by index m = -3, -2, -1, 0 it can be written as a sum:

$$f_{\psi}(x)=\sum_{m=-3}^{m=0}\sum_{n=0}^{2^{-m}-1} a_{mn}\,\psi_{mn}(x)=\sum_{m=-3}^{m=0}\sum_{n=0}^{2^{-m}-1} f_{mn}(x) \qquad (10)$$

Then the first step of approximation is

$$f_{\psi_1}(x) = \sum_{m=-2}^{m=0} \sum_{n=0}^{2^{-m}-1} f_{mn}(x) \qquad (11)$$

$$f_{\psi_1}(x) = f_{-20} + f_{-21} + f_{-22} + f_{-23} + f_{-10} + f_{-11} + f_{00} \qquad (12)$$

in which two component wavelets are equal to zero according to Table 1. The waveforms are presented in Figure 2 (a). Figure 2 (b) presents the result of the second step of approximation in which a few (but not all) wavelets f_{-3n} have been added to the function $f_{\psi 1}(x)$. Function $f_{\psi 2}(x)$ creates a composition of the following wavelets:

$$f_{\psi_2}(x) = f_{-30} + f_{-33} + f_{-34} + f_{-37} + f_{\psi_1}(x) \qquad (13)$$

Analogously it is possible to create successive steps of approximation. All coefficients a_{mn}, for three steps of approximation and calculated according to (7), have been collected in Table 1.

Successive steps of wavelet approximation $f_{\psi k}(x)$ for $k = 1, 2, 3$ have been presented in Figures 2, 3, and 4. The first step of reconstruction creates function $f_{\psi 1}(x)$ as a set of wavelets.

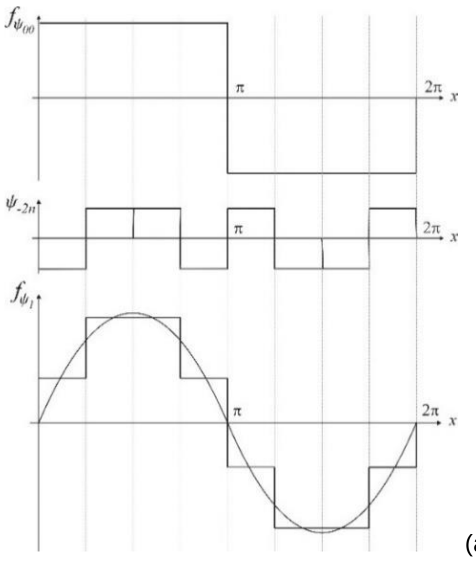

(a)

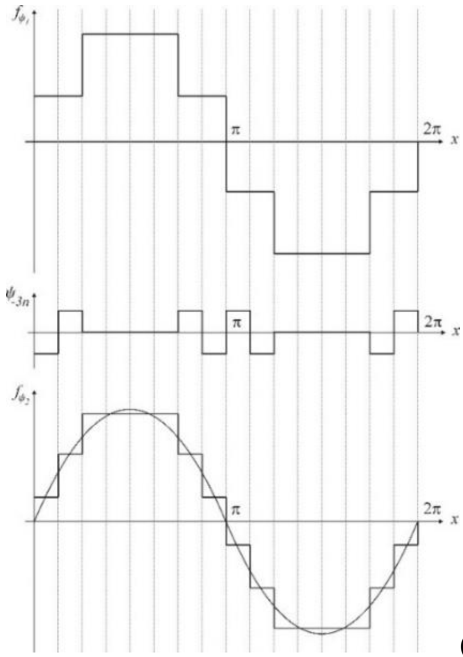

(b)

Fig. 2. The first step of wavelet approximation (a): $f_{\psi_1}(x) = f_{-20} + f_{-21} + f_{-22} + f_{-23} + f_{00}$, and the second step of wavelet approximation (b): $f_{\psi_2}(x) = f_{-30} + f_{-33} + f_{-34} + f_{-37} + f_{\psi 1}$.

Table 1. The wavelet coefficients a_{mn}.

a_{mn}	n					
	0	1	2	3	4	5
a_{0n}	0.636	–	–	–	–	–
a_{-1n}	0	0	–	–	–	–
a_{-2n}	- 0.264	0.264	0.264	- 0.264	–	–
a_{-3n}	- 0.179	- 0.074	0.074	0.179	0.179	0.074

Wavelet converter

One-phase wavelet voltage converter consists of three voltage inverters (respectively transistors T1÷T4, T5÷T8, T9÷T12,) connected in cascade. The proposed method based on wavelet transform is very suitable for cascade converters even though it demands independent voltage sources. In each phase of the complex converter, the component inverters are supplied from three independent voltage sources: U_{D1}, U_{D2}, and U_{D3}. The supply voltages are proportional to the relevant amplitudes of component wavelets. If the proportional factor is set to 500 the voltage U_{D1} = 318 V, U_{D2} = 132 V, and U_{D3} = 84 V.

The control of such a converter is derived from described wavelets model. The inverter control vectors, which were calculated from the Haar wavelet, are shown in Figure 4. The schematic diagram of the one-phase converter is presented in Figure 5. The first inverter, counting from the top, generates the output voltage with the waveform $f_{\psi 00}$, the second with the waveform ψ_{-2n}, and the third with the waveform ψ_{-3n}.

The summing process of the wavelets in the cascade is accomplished by serially connecting the outputs of the component inverters whose switching frequencies differ. Assuming that the fundamental frequency is 50 Hz, the frequencies of individual wavelets are different and take the following values: for $f_{\varphi 00}$ is f = 50 Hz, for ψ_{-2n} is f = 200 Hz, for ψ_{-3n} is f = 400 Hz. For example, for wavelet ψ_{-2n} due to the phase change, there will appear pulses of 5 ms duration two times in each output voltage period. For wavelet ψ_{-3n} pulses of 2.5 ms duration appear.

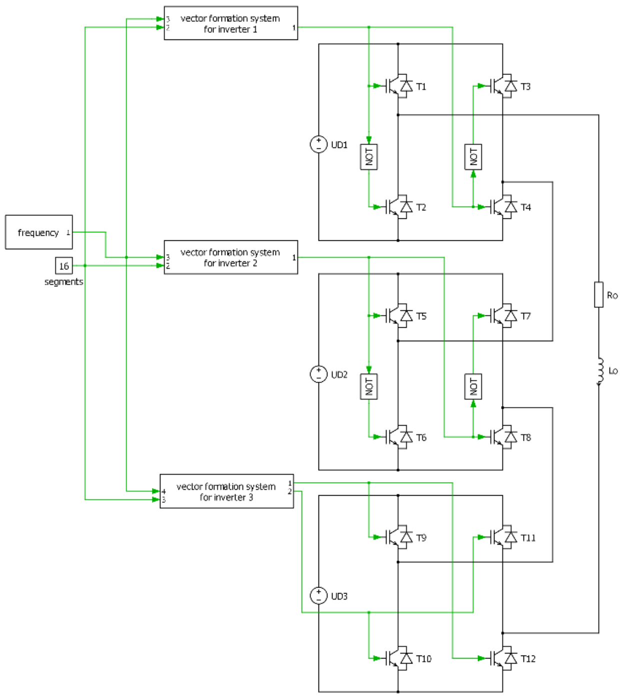

Fig. 3 Scheme of the one phase of the cascaded inverter.

The control principle of three component inverters is presented in Fig. 4. All transistors are controlled by use of simple rectangular pulses. Their amplitudes depend on applied elements.

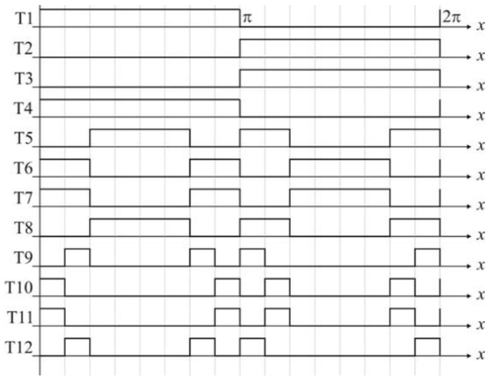

Fig. 4. Control principle of all inverter transistors in one phase of a multi-phase inverter.

The proposed control method based on wavelet transform seems to be very suitable for multi-phase cascade converters even though it demands independent voltage sources. In each phase of the multi-phase complex converter, the component inverters are supplied from three independent voltage sources: U_{D1}, U_{D2}, and U_{D3}. The supply voltages are proportional to the relevant amplitudes of component wavelets. If the proportional factor is set to 500 - what physically relates to 500 V - the supply voltages are:
U_{D1} = 318 V, U_{D2} = 132 V, and U_{D3} = 84 V.

In order to control a multi-phase cascade converter the identical principle of control must be duplicated in every phase and shifted by an angle depended on number of phases. For $\boldsymbol{n}$ phases the displacement $\boldsymbol{\alpha}$ is equal to $\boldsymbol{\alpha} = \frac{2\pi}{n}$. In case of five-phase converter the angle $\boldsymbol{\alpha}$ riches 72°.
The paper shows the shape of the output voltage waveforms acquired during simulation tests. First simulation works were done on the one-phase converter.
The voltage waveforms was achieved according to the rule of three step approximation. So, only the fundamental, first order and the second order wavelets were used to create the output voltage in each of the three phases. According to the authors, the output voltage reproduces the shape of the sinusoidal function with not bad accuracy.
As part of the simulation tests, three-phase voltage and current waveforms for three variants were shown. In the first variant, only the first wavelet form was used. In the second variant, the first and second wavelet forms were used, and in the third variant, three wavelet forms were used. They were mathematically described in the theoretical part of the article.
Simulation tests were carried out in the PLECS program and the RT Box device, which enables HIL (hardware in the loop) simulations. During tests, the cooperation of the proposed inverter with resistive and resistive-inductive loads was checked. With a resistive load, the output voltage and current are similar in shape, so they are not included as a result of the simulation. A more interesting situation occurs with resistive-inductive loads.
Figure 5 shows examples of voltages and current waveforms of the inverter loaded by R_0 = 5 Ω and L_0 = 20 mH connected in series. The fundamental frequency was set as f = 50 Hz. The time constant $\tau = Lo/Ro$ is τ = 4 ms.
The next Figure 6 shows the spectra of waveforms presented in Figure 5.
In these Figures the voltage U_{D1} = 318 V relates to u_1, U_{D2} = 132 V relates to u_2 and U_{D3} = 84 V – u_3. The load parameters are relatively denoted as: U_L - u_0 and I_L – i_0.
The THD factor of the voltage u_1 is the highest and reaches 31%.
The voltages u_2 and u_3 have harmonics of lower amplitudes and higher frequencies. So, the THD_U is significantly lower. Resulting in the output voltage of the converter achieves the THD_U equal to less than 12% while the THD_I – 4,4%. The most considerable third harmonic has the frequency equal to 150 Hz. In spectrum of the voltage waveform U_L one can also notice 5^{th}, 11^{th}, 13^{th} 15^{th} and 17th harmonics – 250, 550, 650 and 750 Hz respectively. In spectrum of the current I_L, the only third harmonic 150 Hz is practically noticeable.

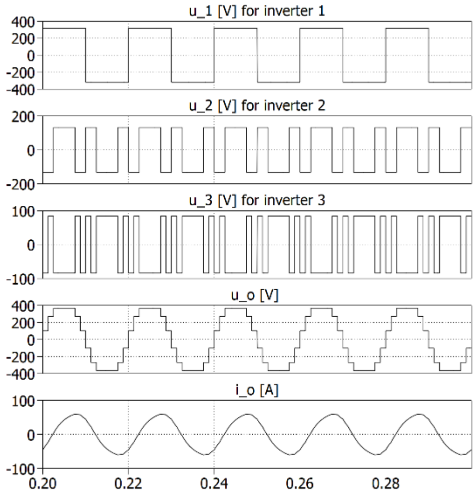

Fig. 5. Voltage waveforms for individual inverters and load voltage and current of the converter (Ro = 5 Ω and Lo = 20 mH).

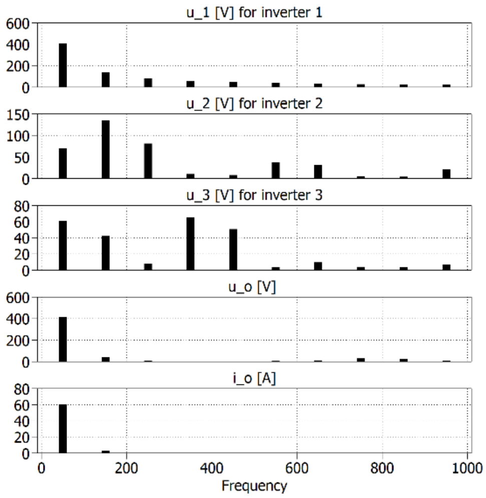

Fig. 6. Spectra of all voltages and load current presented in Figure 5 (Ro = 5 Ω and Lo = 20 mH).

Comparable simulation tests were carried out for the five-phase converter loaded by the same resistive-inductive set of elements in star connection. The fundamental frequency was set also as f = 50 Hz. The time constant of the phase load was the following $\tau = Lo/Ro$ = 4 ms. The cooperation of the proposed converter with such a load was tested. When the load is only resistive the output voltage and current are similar in shape, so the received data were not included.

The simulation results of the converter loaded by R-L set in every phase are presented in Figure 7. Figure 7a presents five wave forms of the control principle and results of the two-step approximation: carrier signal, voltage waveforms of the *inv_1* and *inv_2*, phase-to-phase voltage *u_ba* and phase current *i_a*.

These waveforms prove the suitability of the converter control by use of wavelets. The switching frequency of the component inverters is very low. The inverter *inv_1* works with the output voltage fundamental frequency while the second one *inv_2* demands only three times more switching in one period of the output voltage.

In addition in Figure 7, two time waveforms: the phase-to-phase voltage *u_ba* and phase current *i_a* have been collected

They illustrate the quality of the used two-step approximation.

Next in Figure 7a, all relevant time waveforms taken during simulation tests have been presented. The simulation related to the five-phase converter, so the formula included carrier signal, voltage, and current waveforms in every phase. Additionally, the time waveforms of the phase-to-phase voltage *u_ba*, as well as phase voltage *u_a* and phase *i_a*, have been enclosed. The voltage values (amplitude) are the following: the voltage *u_inv1* = 318 V, *u_inv2* = 132 V.

Figure 7b shows the spectra of time waveforms presented in Figure 7a. Three spectra of the fundamental quantities are selected: the phase-to-phase voltage *u_ba*,, the phase voltage *u_a*, and the phase current *i_a*.

The THD factor of the voltage *u_ba* is high and reaches 31%. Besides the fundamental harmonic, the spectrum includes significant 7^{th} and 9^{th} harmonics (350 and 450 Hz). These significant harmonics appear as also in the phase voltage spectrum but they are poorly visible in the phase current spectrum.

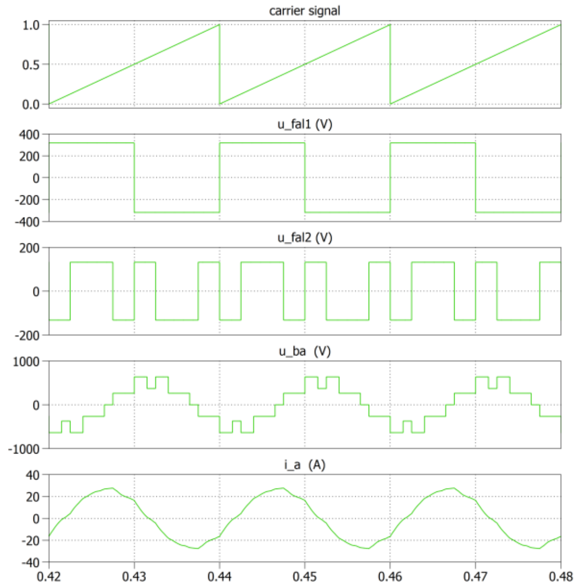

(a)

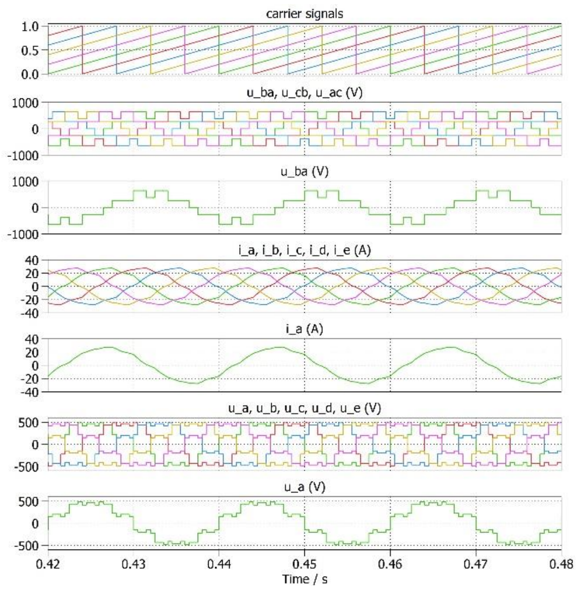

(b)

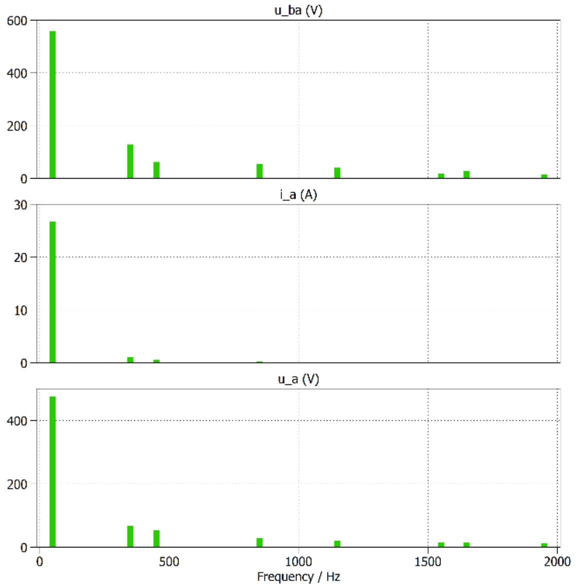

(c)

Fig. 7. Voltage and current waveforms for the first and second step of approximation (a) (b)
and their spectrum (49 harmonics) (b)

Conclusions

The paper examined and proved the possibility of creation multilevel voltage waveforms in the cascaded inverter. The rule of the inverter control is based on the Haar wavelet transform. The paper proves the suitability of this mathematical theory used to inverter control. A simple control circuit and low number of switching in all component two-level inverters permit to reduction the loss power and the content of higher harmonics in the output voltage and current waveforms. The resulting higher harmonics of the output waveforms become easy to filter out. Based on the conducted simulation tests, it was established that acceptable results were obtained already at two component inverters in every phase of the whole cascaded inverter. Adding the third step of approximation it is possible to attain well approximated to sinusoidal wave voltage and current graphs.

References

[1] H.L. Do, A soft-switching DC/DC converter with high voltage gain. IEEE Trans. Power Electron. 2010, 25, 1193–1200. https://doi.org/10.1109/tpel.2009.2039879.
[2] X. Hu, J. Wang, L. Li, Y. Li, A three-winding coupled-inductor DC–DC converter topology with high voltage gain and reduced switch stress. IEEE Trans. Power Electron. 2018, 33, 1453–1462. https://doi.org/10.1109/tpel.2017.2689806.
[3] H. Ramirez, C. Restrepo, T. Konjedic, J. Calvente, A. Romero, C. Baier, R. Giral, Efficiency comparison of fuel-cell hybrid systems based on the noninverting buck-boost converter. IEEE Trans. Power Electron. 2017, 33, pp. 1237–1246.
[4] M.D. Siddique, Low switching frequency based on asymmetrical multilevel inverter topology with reduced switch count. IEEE Access 2019, 7, pp. 86374–86383.
[5] J. Iwaszkiewicz, J. Perz, Multilevel convertors for distributed power generation systems with DC voltage sources; ICREPQ: Saragossa, Spain, 2005.
[6] N.A. Rahim, K. Chaniago, J. Selvaraj, Single-phase seven-level grid connected inverter for photovoltaic system. IEEE Trans. Ind. Electron. 2011, 58, 2435–2443.
[7] J. Liu, X. Zhu, J. Zeng, A seven-level inverter with self-balancing and low voltage stress. IEEE J. Emerg. Sel. Top. Power Electron. 2018, 8, 685–696.
[8] P. Roshankumar, R.S. Kaarthik, K. Gopakumar, J.I. Leon, A seventeen-level inverter formed by cascading flying capacitor and floating capacitor h-bridges. IEEE Trans. Power Electron. 2014, 30, 3471–3478.
[9] E. Drives, A. Maather, P. Electronics, N. Ouest, A novel 31-level packed u cells converter. in proceedings of the 2011 International Conference on Power Engineering, Energy and Electrical Drives, Malaga, Spain, 11–13 May 2011.
[10] J. Iwaszkiewicz , A. Muc, A. Bielecka, Polar voltage space vectors of the six-phase two-level VSI, Energies 2022, 15, 2763. https://doi.org/10.3390/en15082763.
[11] M. Hartman, M. Hashad, J. Iwaszkiewicz, Developing inverter output voltage waveforms with the help of orthogonal space vectors, IEE Conference Power Electronics and Variable Speed Drives PEVD'2000, London, United Kingdom, 18–19 ix 2000.
[12] M. Hashad, J. Iwaszkiewicz, A novel orthogonal-vectors-based topology of multilevel inverters. IEEE Trans. Ind. Electron. 2002, 49, pp. 868–874.
[13] J. Iwaszkiewicz, A novel recurrent approach to the output voltage filtering of the inverter. ELECTR. POWER QUAL UTIL.Pol. Acad. Sci. 2003, 9, pp. 59–65.
[14] A. Muc, J. Iwaszkiewicz, Active filtering of inverter output waveforms based on orthogonal space vector theory, Energies 2022, 7861, https://doi.org/10.3390 /en15217861.
[15] j. Liu, K.W.E. Cheng, Y. Ye, A cascaded multilevel inverter based on switched capacitor for high-frequency AC power distribution system. IEEE Trans. Power Electron. 2014, 29, pp. 4219–4230.
[16] J. Iwaszkiewicz , Mathematical models of power electronics multilevel converters-analysis and applications, Proceedings of Electrotechnical Institute, 227'06, Warsaw, Poland, ISSN-0032-6216.